JPET Fast Forward. Published on September 13, 2012 as DOI: 10.1124/jpet.112.195701
This article has not been copyedited and formatted. The final version may differ from this version.
JPET Fast Forward. Published on September 13, 2012 as DOI: 10.1124/jpet.112.195701

Dendritic spine injury induced by the 8-hydroxy metabolite of Efavirenz

Luis B. Tovar-y-Romo, Namandjé N. Bumpus, Daniel Pomerantz, Lindsay B. Avery, Ned Sacktor, Justin McArthur and Norman J. Haughey

Departments of Neurology, Richard T. Johnson Division of Neuroimmunology and Neurological Infections (L.B.T-y-R., D.P., N.S., J.M., N.J.H.), Pharmacology and Molecular Sciences (N.N.B., L.B.A.) and Psychiatry (N.J.H), The Johns Hopkins University School of Medicine, Baltimore, MD

Running title

Efavirenz metabolites damage neuronal spines

Correspondence. Norman J. Haughey, Department of Neurology, The Johns Hopkins University School of Medicine. Meyer 6-109, 600 North Wolfe Street. Baltimore MD. 21287. email: nhaughe1@jhmi.edu. 443-287-3825 phone. 410-955-0672 fax.

Text pages: 33

Figures: 6

Words in abstract: 241

Words in introduction: 489

Words in discussion: 926

Abbreviations:

ARV, antiretroviral drug; CNS, central nervous system; cART, combination antiretroviral therapies; CYP, cytochrome P450; EFV, Efavirenz; HAD, HIV-associated dementia; HAND, HIV-associated neurocognitive disorders; VOCC, voltage-operated calcium channels.

Recommended section: Toxicology

ABSTRACT

Despite combination antiretroviral therapies (cART), a significant proportion of HIV-infected patients develop HIV-associated neurocognitive disorders (HAND). Ongoing viral replication in the CNS due to poor brain penetration of cART may contribute to HAND. However, it has also been proposed that toxic effects of long-term cART may contribute to HAND. A better understanding of the neurotoxic potential of cART is critically needed in light of the use of CNS penetrating cART to contend with virus reservoir in brain. The Efavirenz (EFV) metabolites 7-hydroxyefavirenz (7-OH-EFV) and 8-hydroxyefavirenz (8-OH-EFV) were synthesized, purified, and chemical structures confirmed by mass spectrometry and NMR. The effects of EFV, 7-OH-EFV and 8-OH-EFV on calcium, dendritic spine morphology, and survival were determined in primary neurons. EFV, 7-OH-EFV and 8-OH-EFV each induced neuronal damage in a dose dependent manner. However, 8-OH-EFV was at-least an order of magnitude more toxic than EFV or 7-OH-EFV, inducing considerable damage to dendritic spines at a 10 nM concentration. The 8-OH-EFV metabolite evoked calcium flux in neurons, which was primarily mediated by L-type voltage operated calcium channels. Blockade of L-type VOCCs protected dendritic spines from 8-OH-EFV-induced damage. Concentrations of EFV and 8-OH-EFV in the cerebral spinal fluid of HIV-infected subjects taking EFV were within the range that damaged neurons in culture. These findings demonstrate that the 8-OH metabolite of EFV is a potent neurotoxin and highlight the importance of directly

determining the effects of antiretroviral drugs, and drug metabolites on neurons and other brain cells.

Introduction

The widespread use of combination antiretroviral therapy (cART) dramatically decreased the mortality rate of HIV-infected individuals, and decreased the incidence of HIV-associated dementia (HAD (Heaton et al., 2011). Although cART decreased the incidence HAD, it appears to have had little impact on the prevalence of milder forms of cognitive impairments that are collectively known as HIV-Associated Neurocognitive Disorders (HAND) (Heaton et al., 2010; Letendre et al., 2010; McArthur et al., 2010; Heaton et al., 2011; Valcour et al., 2011b). Currently available data suggests that 50% of HIV-infected subjects will develop a neurologic disorder (Chang et al., 2004; Ernst and Chang, 2004; Valcour et al., 2004; Chang et al., 2008; Valcour et al., 2011a). Moreover, the occurrence of HAND is associated with an increased risk of death (Vivithanaporn et al., 2010). Although the mechanism(s) for this residual cognitive impairment and association with increased mortality are not completely understood, continued viral replication in the brain due to insufficient central nervous system (CNS) penetration of cART is though to be an underlying mechanism (Robertson et al., 2007). Therefore, cART regimens with increased brain penetration have been proposed to combat HAND (Letendre et al., 2008). While there is evidence that this approach reduces CSF viral load (Marra et al., 2009) and may improve cognitive function(Letendre et al., 2004; Smurzynski et al., 2011), there is also evidence that some antiretroviral drugs (ARVs) are toxic to neurons (Liner et al., 2010), and that ARVs with increased brain penetration are associated with poor cognitive performance (Tozzi et al., 2007; Marra et al., 2009). Therefore, the

effectiveness of brain penetrating cART regimens is currently in question (Koopmans et al., 2009).

Few studies have directly determined the effects of antiretroviral drugs on neuronal function (Schweinsburg et al., 2005; Cardenas et al., 2009), and no studies have determined potential neurotoxic effects of antiretroviral drug metabolites. Most xenobiotics are metabolized by the cytochrome P450 (CYP) superfamily of enzymes that catalyze Phase 1 reactions (oxidation, reduction, hydrolysis). CYPs are concentrated in liver, but are also expressed in brain (Gervot et al., 1999; Bhagwat et al., 2000; Miksys et al., 2003). CNS effects of the non-nucleoside reverse transcriptase inhibitor Efavirenz ((*S*)-(-)-6-chloro-4-(cyclopropylethynyl)-4-(trifluoromethyl)-2,4-dihydro-1H-3,1-benzoxazin-2-one; EFV), have been reported that include sleep disturbances, cognitive and mood disorders(Marzolini et al., 2001; Perez-Molina, 2002; Lochet et al., 2003; Rihs et al., 2006), but to date there are no studies that have directly determined the effects of EFV or its metabolites on neuronal function.

EFV is metabolized primarily by CYP2B6 to produce a series of metabolites of which 8-hydroxyefavirenz (8-OH-EFV) is the most abundant (Ward et al., 2003; Bumpus et al., 2006; Ogburn et al., 2010). In this study we provide evidence that 8-OH-EFV is a potent neurotoxin that dysregulates neuronal calcium homeostasis, and damages dendritic spines in the low nM range. The effects of this metabolite are distinct from the parent drug, and highlight the importance of screening not only antiretroviral medications for neurotoxicity, but also drug metabolites.

METHODS

Human Plasma and CSF. Paired plasma and CSF samples were obtained from 13 HIV-infected subjects enrolled in the North Eastern AIDS Dementia (NEAD) study (Sacktor et al., 2002). All subjects were taking cART regimens that included EFV. Subjects consisted of 10 males and 3 females aged 49.23 ± 10.35 years. CD4+ cell counts in this population were 369.6 ± 110.1 cells/mm^3. HIV was detectable in plasma of 3 subjects, and in CSF of 4 subjects.

Production and isolation of 7-hydroxy and 8-hydroxy efavirenz. P450 2A6 and P450 2B6 cDNAs were co-transformed and expressed with cytochrome P450 reductase in Escherichia coli to produce active P450s (Locuson et al., 2009). EFV (50 µM) was incubated with the membrane preparation for 60 min followed by termination of the reaction using acetonitrile. The samples were spun at 4000 x g for 10 min at 4ºC, supernatant was removed, and the metabolites purified by high pressure liquid chromatography (HPLC) using a Beckman Coulter 4.6 x 250 mm C18 HPLC column. The mobile phase consisted of water 0.1% formic acid (mobile phase A) and acetonitrile 0.1% formic acid (mobile phase B) using a gradient of 55% to 70% B over 24 min.

Following collection of the metabolite containing fractions, the samples were lyophilized and weighed. Methanol was then added to reconstitute the sample such that a 1% 8-hdyroxyefavirenz or 7-hydroxyefavirenz solution was produced. The absorbance of a 1-cm layer of the solution at 247 nm was then measured.

JPET Fast Forward. Published on September 13, 2012 as DOI: 10.1124/jpet.112.195701
This article has not been copyedited and formatted. The final version may differ from this version.

The amount of 8-hydroxyefavirenz was calculated using a molar absorptivity value of 46.5 (specific absorbance: A(1%, 1cm) = 465) and 48.3 (specific absorbance: A(1%, 1cm) = 483) for 7-hydroxyefavirenz.

Quantification of EFV, 7-OH-EFV and 8-OH-EFV. Sample preparation has been previously described (Avery et al., 2010). Briefly, a racemic fluorinated analog of EFV (F-EFV; 10 ng) was added to 50 µl of sample prior to extraction for use as an internal standard. Extraction was conducted using a liquid: liquid method with a 1:1 mixture of hexane and ethyl acetate containing ammonium formate (50 mM). The organic layer was dried and reconstituted in 100 µl of methanol. A fraction of 5 µl was subjected to ultra high performance liquid chromatography tandem mass spectrometry (UPLC-MS-MS) using an AB Sciex QTRAP 5500 mass spectrometer (Foster City, CA) interfaced with an Acquity UPLC equipped with sample and binary solvent managers (Waters, Milford, MA). EFV, 7-OH-EFV, 8-OH-EFV and F-EFV were resolved with a Waters XTerra MS C18, 2.5 µm, 21x50 mm column at a flow rate of 0.5 ml/min using gradient elution of mobile phase A (water, 0.1 % formic acid) to B (acetonitrile, 0.1 % formic acid). Detection was performed in negative ion ESI mode via multiple reaction monitoring (MRM). The following MRM transitions were employed for quantification: m/z 314.0>244.1 (EFV), m/z 329.9>162.0 (8-OH-EFV), m/z 329.9 > 188.9 (7-OH-EFV) m/z 298.0>227.9 (F-EFV). A standard curve was run to simultaneously quantify EFV, 7-OH-EFV and 8-OH-EFV, with a lower quantification limit of 0.5 ng/ml.

Cell Culture. Hippocampal neuronal cultures were prepared from embryonic day 18 Sprague Dawley rats using methods that have been described previously (Wheeler et al., 2009; Xu et al., 2011). In brief, Hippocampi were isolated, trypsinized and cells were dissociated by tituration in a calcium- and magnesium-free Hank's balanced salt solution. Neurons were plated at a density of 150,000 cells/ml on 15 mm diameter polyethylenimine coated glass coverslips in Neurobasal media supplemented with B-27 (Invitrogen, Carlsband CA) and 1% antibiotic solution (10^4 U of penicillin G/ml, 10 mg streptomycin/ml and 25 µg amphotericin B/ml)(Sigma). Three hours after plating, total media was replaced and thereafter was supplemented with Neurobasal media containing B-27 every 7 days. Immunofluorescent staining for microtubule-associated protein 2 (neurons) routinely shows that hippocampal cultures are > 98 % neurons with the remainder of cells predominantly glial fibrillary acidic protein positive astrocytes. Hippocampal cultures were used between 14 and 21 days *in vitro*.

Calcium imaging. Cytosolic calcium levels ($[Ca^{2+}]_c$) were measured using the Ca^{2+}-specific fluorescent probe Fura-2AM. Rat hippocampal neurons were incubated for 20 min with Fura-2AM (2 µM) at 37°C in Neurobasal media containing B27 supplement. Neurons were then washed with Locke's buffer (154 mM NaCl, 3.6 mM $NaHCO_3$, 5.6 mM KCl, 1 mM $MgCl_2$, 5 mM HEPES, 2.3 mM $CaCl_2$, 10 mM glucose; pH 7.4) to remove extracellular Fura-2 and incubated at 37°C for an additional 10 min to allow complete de-esterfication of the probe. Coverslips containing Fura-2 loaded cells were mounted in an RC-26 imaging

chamber (Warner Instruments, Hamden CT) and maintained at 37°C (TC344B Automatic Temperature Controller; Warner instruments Hamden, CT). Neurons were perfused at the rate of 2 ml/min with Locke's buffer using a V8 channel controller (Warner Instruments, Hamden CT). Rapid switching from vehicle to Locke's buffer containing EFV, 7-OH-EFV or 8-OH-EFV was accomplished by placing the perfusion tube and suction apparatus close to the cells to be imaged (with ~ a 0.05 cm gap) so that a thin film of perfusate rapidly passed over the cells. Cells were excited at 340 and 380 nm, and emission was recorded at 510 nm with a video-based intrtacellular imaging system (Photon Technology Inc. Ontario, Canada) equipped with a QuantEM 512sc electron-multiplying gain camera (Photometrics Inc. Tuscon, AZ). Images were acquired at the rate of 200 ms per image pair from cell somas. The fluorescent intensities of ratio images were converted to nM $[Ca^{2+}]_c$ by curve fitting using reference standards as previously described (Wheeler et al., 2009).

Cell survival. Cell viability was determined by nuclear morphology using the fluorescent DNA binding dye Hoescht 33342 as described previously (Haughey et al., 2001). Nuclei were visualized on a Ziess Axiovert 200 inverted microscope (Carl Zeiss microscopy Thornwood NY) under epilfuorescence illumination (340 nm excitation and 510 nm barrier filter) using a 40 X oil immersion objective. Two hundred cells from 5 fields in 3 separate cultures per experimental condition were counted without knowledge of the experimental condition. Cells in which nuclear

staining was diffuse were considered viable and cells where nuclear staining was condensed or fragmented were considered “apoptotic”.

Imaging and quantification of dendritic spines. Dendritic spines were visualized by staining F-actin with phalloidin conjugated to Alexa 568. Neurons were washed once with PBS and fixed with ice-cold 4% PFA for 20 min. Cells were then washed with PBS containing 100 mM glycine, and incubated for 5 min in PBS containing 0.1% Triton X-100, and incubated with phalloidin 568 (5U/ml) for 30 min at room temperature. Coverslips were washed twice with PBS to remove excess probe, and mounted on glass slides using a permanent mounting medium containing anti-fading agents (Vectashield). Dendritic branches were visualized using a Ziess Axiovert 200 inverted microscope (Carl Zeiss microscopy) equipped with an Orca CCD camera (Hamamatsu Photonics) under epilfuorescence illumination (558 nm excitation and 568 nm emission) using a 100 X oil objective.

A minimum of ten neurons from three independent experiments was analyzed for each condition. The number of dendritic spines (defined as thin protrusions emerging from dendritic processes) extending from 2-5 primary dendrites/neuron was quantified for a distance of approximately 20 μm from the cell soma using AxioVision 4.8.2 (Carl Zeiss Inc). Spine density across all measured dendritic segments was normalized to the length of the primary dendrite. Measurements were conducted by an investigator blinded to the experimental condition (D.G.).

RESULTS

The 8-hydroxyefavirenz metabolite evokes calcium influx in neurons.

EFV and the 7-OH-EFV and 8-OH-EFV metabolites used for these studies were isolated by HPLC-fractionation and the structures confirmed using mass spectrometry and NMR according to published spectral information (Mutlib et al., 1999) (Fig 1). We first investigated whether EFV or its hydroxylated metabolites could alter intracellular Ca^{2+} homeostasis in primary rat hippocampal neurons. Two-minute applications of EFV (10 μM), or 7-OH-EFV (10 μM) had no effect on intracellular calcium (Fig 2A-C). However, applications of 8-OH-EFV (10 μM) induced immediate increases of intraneuronal Ca^{2+} (Fig 2D). With a 10 μM dose of 8-OH-EFV, approximately half of the neurons appeared undergo a catastrophic loss of membrane integrity and release of the calcium probe. The remaining neurons exhibited clear signs of damage including beading of neurites and vacuolization of the soma (data not shown). We then conducted a dose response for 8-OH-EFV (0.1-10 μM) and found that 1 μM was the minimum effective dose to consistently increase intraneuronal Ca^{2+} (Fig 2E) within 1-5 sec of application (Fig 2E inset). Applications of 8-OH-EFV induced the entry of calcium from an extracellular source, since the removal calcium from the buffer blocked this effect (Fig 2F, G).

To determine the mechanism of Ca^{2+} influx we used pharmacological inhibitors to block the major calcium permeable ion channels in neurons including NMDA (MK-801; 20 μM), AMPA (NBQX; 20 μM), purinergic (PPADS; 10 μM and Suramin; 100 μM), or voltage-gated calcium channels (VOCC; nifedipine; 10 μM)

and exposed neurons to 8-OH-EFV (1 μM; Fig 3A). Blockade of NMDA or AMPA receptors had no effects on 8-OH-EFV-induced calcium influx (Fig 3B-C). Blockade of purinergic receptors (Fig 3D, E), or VOCC (Fig 3F) each partially reduced 8-OH-EFV-evoked calcium influx. Blocking both purinergic receptors and VOCC slowed the rise of intraneuronal Ca^{2+} that followed 8-OH-EFV exposures, but resulted in a similar peak level within 100 sec. compared with either drug alone (Figure 3G).

8-hydroxyefavirenz is potent neurotoxin.

We exposed primary neuronal cultures to EFV, 7-OH-EFV, or 8-OH-EFV (0.01-10 μM) for 24 h and determined apoptosis by nuclear morphology using the fluorescent DNA binding dye Hoescht 33342. The dose-response relationships for EFV and 7-OH-EFV were similar, with each compound exhibiting a minimum toxic dose of 0.1 μM that produced 41.3 ± 14.0% (EFV), and 41.2 ± 15.0 % (7-OH EFV) increases in apoptotic nuclei (Fig 4). At the highest dose tested (10 μM) EFV produced a 66.6 ± 4.2% and 7-OH-EFV produced a 63.5 ± 12.2 % increase in apoptotic nuclei (Fig 4A) In contrast, 8-OH-EFV was at-least an order of magnitude more toxic, and increased the percent of apoptotic nuclei to 36.4% ± 7.1% at a 0.01 μM dose (Fig 4A). Neurotoxicity induced by 8-OH-EFV was not prevented by inhibition of purinergic receptors with PPADS (37.9 ± 11.8 % death), but was partially prevented by inhibition of L-type VOCCs (24.5 ± 8.0 % death). Inhibition of both purinergic receptors and L-type VOCCs did not further improve neuronal survival (27.6 ± 8.0; Fig. 4B).

We next determined if low concentrations of EFV, or its hydroxylated metabolites (0.01 and 0.1 μM) damaged dendritic spines. EFV and the metabolites 7-OH-EFV and 8-OH-EFV each produced considerable loss of dendritic spines at a 0.1 μM dose. In control conditions there were 9.5 ± 0.9 secondary dendrites per 10 μm. Spine density was reduced to 4.0 ± 1.4 for EFV, 4.9 ± 1.5 for 7-OH-EFV, and to 4.7 ± 1.6 for 8-OH-EFV with a 0.1 μM dose. In contrast, the 8-OH metabolite of EFV was considerably more toxic, and reduced the number of dendritc spines to 5.2 ± 1.7 per 10 μm at a dose of 0.01 μM (Fig 5B). EFV and 7-OH-EFV at the dose of 0.001 μM did not appreciably alter the number of dendritic spines (Fig 5A). Blockade of purinergic receptors with PPADS did not rescue dendritic spine damage induced by 8-OH-EFV (5.2 ± 2.0 per 10 μm), while inhibition of L-type VOCCs with nifedipine partially protected from 8-OH-EFV induced spine loss (8.9 ± 2.4 per 10 μm)(Fig 5B). Inhibition of both purinergic receptors and VOCCs did not offer additional protection (7.5 ± 2.2 per 10 μm) compared with inhibition of VOCCs alone (Fig 5B). These data demonstrate that the EFV metabolite 8-OH-EFV in the low nM range induces damage to dendritic spines.

Plasma and CSF concentrations of Efavirenz and 8-hydroxyefavirenz

We determined plasma and CSF concentrations of EFV and 8-OH-EFV in human subjects on stable cART regimens that included EFV. In these subjects the median plasma concentration of EFV was 2170 ng/ml (range 1010-7510), and 166 ng/ml (range 69.3-621) for 8-OH-EFV (Fig 6A). The median CSF

concentration of EFV was 18.8 ng/ml (range 6.28-52.9) and 3.37 (range 0.35-32.7) for 8-OH-EFV (Fig 6B). These median values correspond to CSF concentrations of 59.6 nM for EFV and 10.2 nM for 8-OH-EFV.

DISCUSSION

Long-term cART has dramatically decreased the mortality rate of HIV-infected individuals, owing to the ability of these drugs to suppress viral replication. Most ARVs do not enter into the CNS in appreciable amounts, and thus brain has remained a reservoir for HIV (Langford et al., 2006). Ongoing (although likely low-level) viral replication in brain is thought to contribute to the pathogenesis of HAND (Masliah et al., 2000; Neuenburg et al., 2002; Langford et al., 2003) and targeting ARVs to inhibit viral replication in brain to treat or prevent HAND has been suggested (May et al., 2007). However, this approach has raised concerns that some ARVs may damage neurons. Unfortunately, very little experimental data is available on the potential of ARVs or drug metabolites to damage neurons.

The CNS side effects of EFV that have been described include dizziness, vivid dreams, headaches, disturbances in attention and sleep, psychotic events and hallucinations, with the majority of these events regarded as mild. The most evident CNS side effects of EFV generally occur and resolve within the first month of therapy and rarely lead to discontinuation of the therapy (Moyle, 1999). However, recent data have associated EFV with a higher risk of neurocognitive impairment, particularly on tasks requiring a high degree of attention and

executive function (Ciccarelli et al., 2011). It has also been reported that cART regimens containing EFV may lead to a worsening of cognitive performance after several weeks of treatment (Winston et al., 2010), and that these impairments in cognitive performance are significantly improved when patients discontinued treatment (Robertson et al., 2010). As would be expected, the severity of these CNS symptoms correlates to EFV plasma concentrations (Marzolini et al., 2001). However not all studies have confirmed this relationship (Clifford et al., 2005).

In this study we sought to directly determine the effects of EFV and its hydroxylated metabolites on neurons. Our findings suggest that 8-OH-EFV is at-least an order of magnitude more toxic to neurons compared to the parent compound EFV or 7-OH-EFV. Damage to dendritic spines was produced with 100 nM EFV or 7-OH-EFV. The 8-OH-EFV metabolite was approximately 10-fold more toxic compared to EFV and caused considerable dendritic damage10 nM with frank cell death at a 100 nM dose. We found that concentrations of EFV and 8-OH-EFV in CSF from human subjects taking cART appear to be within this neurotoxic dose range. The median concentration of EFV in the CSF of HIV-infected subjects taking cART-containing EFV was 59.6 nM, similar to previously reported CSF concentrations of 35 nM (0.5% of that in plasma) (Moyle, 1999; Tashima et al., 1999; Best et al., 2011). The median concentration of 8-OH-EFV in CSF was 10.2 nM. Together these data suggest that concentrations of the parent drug EFV in brain may be within the range that can damage neurons, and that concentrations of 8-OH-EFV could be three times the minimal dose that produced dendritic damage to cultured neurons. Moreover, there may be a

genetic susceptibility to the neurotoxic effects of EFV that is related to its rate of metabolism. Extensive EFV metabolizers were recently identified who express the *1/1 haplotype of CYP2B6 (Ngaimisi et al., 2010). Thus, a genetic susceptibility in some individuals may exaggerate the neurotoxic effects of EFV due to a rapid metabolism of EFV with accumulations of the 8-OH-EFV metabolite.

This enhanced toxicity of 8-OH-EFV appears to be due to the ability of this metabolite to perturb calcium homeostasis. The 8-OH-EFV metabolite, but not 7-OH-EFV or the parent compound EFV induced rapid calcium influx in neurons that was partially inhibited by a general antagonist of purinergic receptors, and was almost completely eliminated by blockade of L-type VOCC. Calcium permeable NMDA and AMPA-type glutamate receptors were not activated by 8-OH-EFV. Consistent with a prominent role for VOCCs, inhibition of L-type calcium channels partially protected densritic spines from 8-OH-EFV-induced damage. These data suggest that the metabolism of EFV produces a highly neurotoxic metabolite (8-OH-EFV) that is capable of damaging neurites at very low concentration. Thus, cognitive impairments associated with EFV may involve synaptic damage mediated by its major metabolite 8-OH-EFV. It is interesting to note that the parent compound EFV, and the 7-OH-EFV metabolite also displayed a neurotoxic potential that appeared to be calcium-independent. The mechanisms of these separate toxic effects are currently being studied and may interact with the toxicity produced by 8-OH-EFV.

It is interesting that position of the OH group on the 7 vs 8 carbon of the benzoxazine ring produces such a dramatic difference in evoked calcium flux and neurotoxicity. These data suggest that the proximity of the OH group at position 8 to the nitrogen group in the benzoxazine structure is the critical determinant for forming a highly neurotoxic metabolite of EFV. Therefore, substituting the carbon at position 8 so that EFV cannot be hydroxylated at this position should produce a compound with decreased neurotoxicity. Such a drug with a fluorine substituent at carbon 8 which retains inhibitory activity at reverse transcriptase (with an IC_{90} = 7.19 nM that is close to the IC_{90} = 2.03 nM of EFV) has been synthesized (Patel et al., 1999). This drug may offer an alternative to EFV with reduced neurotoxicity resulting from secondary metabolite production.

These findings contribute to our understanding of the mechanism for neurotoxicity associated with EFV therapy. Since the anticipated length of therapy for cART is the lifetime of the patient, these data highlight the importance of screening antiretroviral drugs and drug metabolites for neurotoxic potential. This principle may be especially important if brain penetration is desired to reduce CNS viral replication.

Authorship contributions:

Participated in research design: Haughey, Tovar-y-Romo, McArthur, Sacktor.

Conducted experiments: Tovar-y-Romo, Bumpus, Pomerantz, Avery.

Contributed reagents and analytic tools: Bumpus.

Performed data analysis: Tovar-y-Romo, Haughey, Bumpus, Avery.

Wrote the manuscript: Tovar-y-Romo, Haughey.

References

Avery LB, Parsons TL, Meyers DJ and Hubbard WC (2010) A highly sensitive ultra performance liquid chromatography-tandem mass spectrometric (UPLC-MS/MS) technique for quantitation of protein free and bound efavirenz (EFV) in human seminal and blood plasma. *J Chromatogr B Analyt Technol Biomed Life Sci* **878**:3217-3224.

Best BM, Koopmans PP, Letendre SL, Capparelli EV, Rossi SS, Clifford DB, Collier AC, Gelman BB, Mbeo G, McCutchan JA, Simpson DM, Haubrich R, Ellis R and Grant I (2011) Efavirenz concentrations in CSF exceed IC50 for wild-type HIV. *J Antimicrob Chemother* **66**:354-357.

Bhagwat SV, Boyd MR and Ravindranath V (2000) Multiple forms of cytochrome P450 and associated monooxygenase activities in human brain mitochondria. *Biochem Pharmacol* **59**:573-582.

Bumpus NN, Kent UM and Hollenberg PF (2006) Metabolism of efavirenz and 8-hydroxyefavirenz by P450 2B6 leads to inactivation by two distinct mechanisms. *J Pharmacol Exp Ther* **318**:345-351.

Cardenas VA, Meyerhoff DJ, Studholme C, Kornak J, Rothlind J, Lampiris H, Neuhaus J, Grant RM, Chao LL, Truran D and Weiner MW (2009) Evidence for ongoing brain injury in human immunodeficiency virus-positive patients treated with antiretroviral therapy. *J Neurovirol* **15**:324-333.

Chang L, Lee PL, Yiannoutsos CT, Ernst T, Marra CM, Richards T, Kolson D, Schifitto G, Jarvik JG, Miller EN, Lenkinski R, Gonzalez G and Navia BA (2004) A

multicenter in vivo proton-MRS study of HIV-associated dementia and its relationship to age. *Neuroimage* **23**:1336-1347.

Chang L, Wong V, Nakama H, Watters M, Ramones D, Miller EN, Cloak C and Ernst T (2008) Greater than age-related changes in brain diffusion of HIV patients after 1 year. *J Neuroimmune Pharmacol* **3**:265-274.

Ciccarelli N, Fabbiani M, Di Giambenedetto S, Fanti I, Baldonero E, Bracciale L, Tamburrini E, Cauda R, De Luca A and Silveri MC (2011) Efavirenz associated with cognitive disorders in otherwise asymptomatic HIV-infected patients. *Neurology* **76**:1403-1409.

Clifford DB, Evans S, Yang Y, Acosta EP, Goodkin K, Tashima K, Simpson D, Dorfman D, Ribaudo H and Gulick RM (2005) Impact of efavirenz on neuropsychological performance and symptoms in HIV-infected individuals. *Ann Intern Med* **143**:714-721.

Ernst T and Chang L (2004) Effect of aging on brain metabolism in antiretroviral-naive HIV patients. *AIDS* **18 Suppl 1**:S61-67.

Gervot L, Rochat B, Gautier JC, Bohnenstengel F, Kroemer H, de Berardinis V, Martin H, Beaune P and de Waziers I (1999) Human CYP2B6: expression, inducibility and catalytic activities. *Pharmacogenetics* **9**:295-306.

Haughey NJ, Nath A, Mattson MP, Slevin JT and Geiger JD (2001) HIV-1 Tat through phosphorylation of NMDA receptors potentiates glutamate excitotoxicity. *J Neurochem* **78**:457-467.

Heaton RK, Clifford DB, Franklin DR, Jr., Woods SP, Ake C, Vaida F, Ellis RJ, Letendre SL, Marcotte TD, Atkinson JH, Rivera-Mindt M, Vigil OR, Taylor MJ,

Collier AC, Marra CM, Gelman BB, McArthur JC, Morgello S, Simpson DM, McCutchan JA, Abramson I, Gamst A, Fennema-Notestine C, Jernigan TL, Wong J and Grant I (2010) HIV-associated neurocognitive disorders persist in the era of potent antiretroviral therapy: CHARTER Study. *Neurology* **75**:2087-2096.

Heaton RK, Franklin DR, Ellis RJ, McCutchan JA, Letendre SL, Leblanc S, Corkran SH, Duarte NA, Clifford DB, Woods SP, Collier AC, Marra CM, Morgello S, Mindt MR, Taylor MJ, Marcotte TD, Atkinson JH, Wolfson T, Gelman BB, McArthur JC, Simpson DM, Abramson I, Gamst A, Fennema-Notestine C, Jernigan TL, Wong J and Grant I (2011) HIV-associated neurocognitive disorders before and during the era of combination antiretroviral therapy: differences in rates, nature, and predictors. *J Neurovirol* **17**:3-16.

Koopmans PP, Ellis R, Best BM and Letendre S (2009) Should antiretroviral therapy for HIV infection be tailored for intracerebral penetration? *Neth J Med* **67**:206-211.

Langford D, Marquie-Beck J, de Almeida S, Lazzaretto D, Letendre S, Grant I, McCutchan JA, Masliah E and Ellis RJ (2006) Relationship of antiretroviral treatment to postmortem brain tissue viral load in human immunodeficiency virus-infected patients. *J Neurovirol* **12**:100-107.

Langford TD, Letendre SL, Larrea GJ and Masliah E (2003) Changing patterns in the neuropathogenesis of HIV during the HAART era. *Brain Pathol* **13**:195-210.

Letendre S, Marquie-Beck J, Capparelli E, Best B, Clifford D, Collier AC, Gelman BB, McArthur JC, McCutchan JA, Morgello S, Simpson D, Grant I and Ellis RJ (2008) Validation of the CNS Penetration-Effectiveness rank for quantifying antiretroviral penetration into the central nervous system. *Arch Neurol* **65**:65-70.

Letendre SL, Ellis RJ, Ances BM and McCutchan JA (2010) Neurologic complications of HIV disease and their treatment. *Top HIV Med* **18**:45-55.

Letendre SL, McCutchan JA, Childers ME, Woods SP, Lazzaretto D, Heaton RK, Grant I and Ellis RJ (2004) Enhancing antiretroviral therapy for human immunodeficiency virus cognitive disorders. *Ann Neurol* **56**:416-423.

Liner J, Meeker RB and Robertson K (2010) CNS toxicity of antiretroviral drugs, in *17th Conference on Retrovirus and Opportunistic Infections* San Francisco, CA.

Lochet P, Peyriere H, Lotthe A, Mauboussin JM, Delmas B and Reynes J (2003) Long-term assessment of neuropsychiatric adverse reactions associated with efavirenz. *HIV Med* **4**:62-66.

Locuson CW, Ethell BT, Voice M, Lee D and Feenstra KL (2009) Evaluation of Escherichia coli membrane preparations of canine CYP1A1, 2B11, 2C21, 2C41, 2D15, 3A12, and 3A26 with coexpressed canine cytochrome P450 reductase. *Drug Metab Dispos* **37**:457-461.

Marra CM, Zhao Y, Clifford DB, Letendre S, Evans S, Henry K, Ellis RJ, Rodriguez B, Coombs RW, Schifitto G, McArthur JC and Robertson K (2009) Impact of combination antiretroviral therapy on cerebrospinal fluid HIV RNA and neurocognitive performance. *AIDS* **23**:1359-1366.

Marzolini C, Telenti A, Decosterd LA, Greub G, Biollaz J and Buclin T (2001) Efavirenz plasma levels can predict treatment failure and central nervous system side effects in HIV-1-infected patients. *AIDS* **15**:71-75.

Masliah E, DeTeresa RM, Mallory ME and Hansen LA (2000) Changes in pathological findings at autopsy in AIDS cases for the last 15 years. *AIDS* **14**:69-74.

May S, Letendre S, Haubrich R, McCutchan JA, Heaton R, Capparelli E and Ellis R (2007) Meeting practical challenges of a trial involving a multitude of treatment regimens: an example of a multi-center randomized controlled clinical trial in neuroAIDS. *J Neuroimmune Pharmacol* **2**:97-104.

McArthur JC, Steiner J, Sacktor N and Nath A (2010) Human immunodeficiency virus-associated neurocognitive disorders: Mind the gap. *Ann Neurol* **67**:699-714.

Miksys S, Lerman C, Shields PG, Mash DC and Tyndale RF (2003) Smoking, alcoholism and genetic polymorphisms alter CYP2B6 levels in human brain. *Neuropharmacology* **45**:122-132.

Moyle GJ (1999) Efavirenz: shifting the HAART paradigm in adult HIV-1 infection. *Expert Opin Investig Drugs* **8**:473-486.

Mutlib AE, Chen H, Nemeth GA, Markwalder JA, Seitz SP, Gan LS and Christ DD (1999) Identification and characterization of efavirenz metabolites by liquid chromatography/mass spectrometry and high field NMR: species differences in the metabolism of efavirenz. *Drug Metab Dispos* **27**:1319-1333.

Neuenburg JK, Brodt HR, Herndier BG, Bickel M, Bacchetti P, Price RW, Grant RM and Schlote W (2002) HIV-related neuropathology, 1985 to 1999: rising prevalence of HIV encephalopathy in the era of highly active antiretroviral therapy. *J Acquir Immune Defic Syndr* **31**:171-177.

Ngaimisi E, Mugusi S, Minzi OM, Sasi P, Riedel KD, Suda A, Ueda N, Janabi M, Mugusi F, Haefeli WE, Burhenne J and Aklillu E (2010) Long-term efavirenz autoinduction and its effect on plasma exposure in HIV patients. *Clin Pharmacol Ther* **88**:676-684.

Ogburn ET, Jones DR, Masters AR, Xu C, Guo Y and Desta Z (2010) Efavirenz primary and secondary metabolism in vitro and in vivo: identification of novel metabolic pathways and cytochrome P450 2A6 as the principal catalyst of efavirenz 7-hydroxylation. *Drug Metab Dispos* **38**:1218-1229.

Patel M, Ko SS, McHugh RJ, Jr., Markwalder JA, Srivastava AS, Cordova BC, Klabe RM, Erickson-Viitanen S, Trainor GL and Seitz SP (1999) Synthesis and evaluation of analogs of Efavirenz (SUSTIVA) as HIV-1 reverse transcriptase inhibitors. *Bioorg Med Chem Lett* **9**:2805-2810.

Perez-Molina JA (2002) Safety and tolerance of efavirenz in different antiretroviral regimens: results from a national multicenter prospective study in 1,033 HIV-infected patients. *HIV Clin Trials* **3**:279-286.

Rihs TA, Begley K, Smith DE, Sarangapany J, Callaghan A, Kelly M, Post JJ and Gold J (2006) Efavirenz and chronic neuropsychiatric symptoms: a cross-sectional case control study. *HIV Med* **7**:544-548.

Robertson KR, Smurzynski M, Parsons TD, Wu K, Bosch RJ, Wu J, McArthur JC, Collier AC, Evans SR and Ellis RJ (2007) The prevalence and incidence of neurocognitive impairment in the HAART era. *AIDS* **21**:1915-1921.

Robertson KR, Su Z, Margolis DM, Krambrink A, Havlir DV, Evans S and Skiest DJ (2010) Neurocognitive effects of treatment interruption in stable HIV-positive patients in an observational cohort. *Neurology* **74**:1260-1266.

Sacktor N, McDermott MP, Marder K, Schifitto G, Selnes OA, McArthur JC, Stern Y, Albert S, Palumbo D, Kieburtz K, De Marcaida JA, Cohen B and Epstein L

(2002) HIV-associated cognitive impairment before and after the advent of combination therapy. *J Neurovirol* **8**:136-142.

Schweinsburg BC, Taylor MJ, Alhassoon OM, Gonzalez R, Brown GG, Ellis RJ, Letendre S, Videen JS, McCutchan JA, Patterson TL and Grant I (2005) Brain mitochondrial injury in human immunodeficiency virus-seropositive (HIV+) individuals taking nucleoside reverse transcriptase inhibitors. *J Neurovirol* **11**:356-364.

Smurzynski M, Wu K, Letendre S, Robertson K, Bosch RJ, Clifford DB, Evans S, Collier AC, Taylor M and Ellis R (2011) Effects of central nervous system antiretroviral penetration on cognitive functioning in the ALLRT cohort. *AIDS* **25**:357-365.

Tashima KT, Caliendo AM, Ahmad M, Gormley JM, Fiske WD, Brennan JM and Flanigan TP (1999) Cerebrospinal fluid human immunodeficiency virus type 1 (HIV-1) suppression and efavirenz drug concentrations in HIV-1-infected patients receiving combination therapy. *J Infect Dis* **180**:862-864.

Tozzi V, Balestra P, Bellagamba R, Corpolongo A, Salvatori MF, Visco-Comandini U, Vlassi C, Giulianelli M, Galgani S, Antinori A and Narciso P (2007) Persistence of neuropsychologic deficits despite long-term highly active antiretroviral therapy in patients with HIV-related neurocognitive impairment: prevalence and risk factors. *J Acquir Immune Defic Syndr* **45**:174-182.

Valcour V, Paul R, Neuhaus J and Shikuma C (2011a) The Effects of Age and HIV on Neuropsychological Performance. *J Int Neuropsychol Soc* **17**:190-195.

Valcour V, Shikuma C, Shiramizu B, Watters M, Poff P, Selnes O, Holck P, Grove J and Sacktor N (2004) Higher frequency of dementia in older HIV-1 individuals: the Hawaii Aging with HIV-1 Cohort. *Neurology* **63**:822-827.

Valcour V, Sithinamsuwan P, Letendre S and Ances B (2011b) Pathogenesis of HIV in the central nervous system. *Curr HIV/AIDS Rep* **8**:54-61.

Vivithanaporn P, Heo G, Gamble J, Krentz HB, Hoke A, Gill MJ and Power C (2010) Neurologic disease burden in treated HIV/AIDS predicts survival: a population-based study. *Neurology* **75**:1150-1158.

Ward BA, Gorski JC, Jones DR, Hall SD, Flockhart DA and Desta Z (2003) The cytochrome P450 2B6 (CYP2B6) is the main catalyst of efavirenz primary and secondary metabolism: implication for HIV/AIDS therapy and utility of efavirenz as a substrate marker of CYP2B6 catalytic activity. *J Pharmacol Exp Ther* **306**:287-300.

Wheeler D, Knapp E, Bandaru VV, Wang Y, Knorr D, Poirier C, Mattson MP, Geiger JD and Haughey NJ (2009) Tumor necrosis factor-alpha-induced neutral sphingomyelinase-2 modulates synaptic plasticity by controlling the membrane insertion of NMDA receptors. *J Neurochem* **109**:1237-1249.

Winston A, Duncombe C, Li PC, Gill JM, Kerr SJ, Puls R, Petoumenos K, Taylor-Robinson SD, Emery S and Cooper DA (2010) Does choice of combination antiretroviral therapy (cART) alter changes in cerebral function testing after 48 weeks in treatment-naive, HIV-1-infected individuals commencing cART? A randomized, controlled study. *Clin Infect Dis* **50**:920-929.

Xu H, Bae M, Tovar-y-Romo LB, Patel N, Bandaru VV, Pomerantz D, Steiner JP and Haughey NJ (2011) The Human Immunodeficiency Virus Coat Protein gp120 Promotes Forward Trafficking and Surface Clustering of NMDA Receptors in Membrane Microdomains. *J Neurosci* **31**:17074-17090.

Footnotes

This work was supported by the National Institutes of Health grants [AA0017408], [MH077542], [MH075673], [AG034849], [MH075673], [MH71150], and [NS049465].

Figure Captions

Figure 1. MS/MS spectra and fragmentation pattern of hydroxylated metabolites of EFV. The hydroxylated metabolites 7-OH-EFV and 8-OH-EFV were collected by fractionation following incubation of EFV with membrane preparations expressing CYPs 2A6 and 2B6. Hydroxylated EFV metabolites were fragmented and identified by triple quarudpole mass spectrometry. **A)** 7-OH-EFV fragments (m/z 330/258 and m/z 330/286). **B)** 8-OH-EFV fragments (m/z 330/210, m/z 330/246, m/z 330/250, m/z 330/258 and m/z 330/286).

Figure 2. **Calcium responses in neurons exposed to EFV and hydroxylated metabolites.** Primary hippocampal neurons were loaded with the calcium-sensitive dye fura-2 AM and images were acquired in neuronal somas at a rate of one image pair per second. Panels show the average ± S.D. of intracellular calcium concentrations over the indicated times. Arrows indicate the addition of **A)** vehicle, **B)** EFV, **C)** 7-OHEFV, and **D)** 8-OHEFV (each at 10 μM). **E**) Dose-response relationship showing the intracellular calcium response to 8-OH-EFV (0.1 - 10 μM). Inset shows the neuronal calcium response to 1 μM 8-OH-EFV. **F)** Removing calcium from the perfusion buffer blunted the neuronal calcium response to 8-OH-EFV (10 μM), suggesting that intracellular calcium increases were largely due to the influx of extracellular calcium. **G**) Summary data showing average peak intracellular calcium increases evoked by EFV, 7-OH-EFV and 8-OH-EFV (each at a concentration of 10 μM). Quantitative data are the average ± SD of 20–25 neurons derived from five separate experiments. ANOVA with

Tukey's *post hoc* comparisons. *** = $p < 0.001$ compared with control; ### = $p < 0.001$ compared with 8-OHEFV.

Figure 3. **8-OH-EFV-evoked calcium increases neurons involves voltage operated calcium channels and purinergic receptors**. The source of 8-OH-EFV-evoked calcium influx in neurons was determined using pharmacological inhibitors to block specific calcium permeable channels. Panels show the average ± SD of intracellular calcium concentration over the indicated time. Arrows indicate the addition of 8-OH-EFV (1 μM) in neurons treated with **(A)** vehicle, **(B)** the NMDA antagonist MK-801 (10 μM), **C)** the AMPA receptor blocker NBQX (10 μM), **D)** the general purinergic receptor antagonists suramine (100 μM), or **E)** PPADS (10 μM), **F)** the voltage operated calcium channel antagonist nifedipine (10 μM), and **G)** combination of PPADS and nifedipine. **H)** Summary data of average peak intracellular calcium increases for the indicated experimental conditions. Quantitative data are the average ± SD of 20–25 neurons from five separate experiments. ANOVA with Tukey's *post hoc* comparisons. * = $p < 0.05$; ** = $p < 0.01$ compared with control.

Figure 4. **Dose effects of EFV, 7-OH-EFV and 8-OH-EFV on neuronal survival.** Neurons were incubated with EFV, 7-OH-EFV and 8-OH-EFV (0.01 - 10 μM) for 24 h and the number of nuclei with apoptotic morphology were quantified. **A)** Representative images of primary neurons for the indicated experimental conditions labeled with Hoescht33342 (1 μM). This dye labels

chromatin and appears diffuse in healthy nuclei and appears condensed or fragmented (arrows indicate examples) in apoptotic nuclei. **B)** Dose-response survival curves for EFV (circles, continuous line), 7-OHEFV (squares, dotted line), and 8-OHEFV (triangles, dashed line). Each compound decreased neuronal survival in a dose dependent manner, with 8-OH-EFV showing the most potent effects on neuronal survival at each dose tested. Inset shows the main effect of 8-OH-EFV compared with EFV (One-way ANOVA; $p < 0.0001$). **C)** Neuronal apoptosis elicited by 8-OH-EFV (100 nM) was not prevented by the purinergic receptor antagonist PPADS (10 μM), but was reversed by the voltage operated calcium channel antagonist nifedipine (10 μM). The combination of PPADS and nifedipine showed a neuroprotective effect similar to nifedipine alone. Data represent the average ± S.D. of 200 cells from a total of three separate experiments per condition. ANOVA with Tukey's *post hoc* comparisons. *** = $p < 0.001$, ** = $p < 0.01$ compared with control, # = $p < 0.05$ compared with 8-OH-EFV.

Figure 5. Dose effects of EFV, 7-OH-EFV and 8-OH-EFV on dendritic spines. Neurons were treated for 24 h with the indicated concentrations of EFV, 7-OH-EFV, or 8-OH-EFV and dendritic spines were visualized by labeling F-actin with a fluorescent phalloidin. **A)** Micrographs showing the loss of dendritic spines in neurons treated with the indicated concentrations of EFV, 7-OH-EFV and 8-OH-EFV. Arrows indicate examples of spines. Scale bar indicates 5 μm. Quantitative analysis shows that 8-OH-EFV damages dendritic spines at a lower dose (10

nM) compared with EFV or 7-OH-EFV. **B)** Example micrographs showing dendrites and dendritic spines following exposures for 24 h to vehicle (control), 8-OH-EFV (100 nM), alone or in combination with the general purinergic receptor antagonist PPADS (10 μM), the L-type voltage operated calcium channel antagonist nifedipine (10 μM), or both drugs combined. Summary data shows that nifedipine, but not PPADS effectively protects dendritic spines from 8-OH-EFV-induced damage. Quantitative data are the average ± S.D. of the number of dendritic spines from a total of 10 different neurons in each of 3 independent experiments per condition. ANOVA with Tukey's *post hoc* comparisons. *** = $p < 0.001$, ** = $p < 0.01$ compared with control, ### = $p < 0.001$, # = $p < 0.05$ compared with 8-OH-EFV.

Figure 6. Concentrations of EFV and 8-OH-EFV in plasma and CSF. Matched plasma and CSF samples were collected from 13 subjects taking cART regimens that contained EFV. Concentrations of EFV and 8-OH-EFV in **A)** plasma and **B)** CSF are shown for each subject. Cross bars indicates median concentrations.

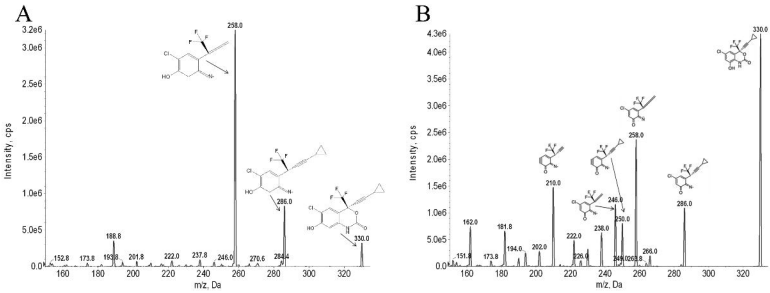
A
B
Intensity, cps
m/z, Da
3.2e6
3.0e6
2.5e6
2.0e6
1.5e6
1.0e6
5.0e5
0.0
4.3e6
4.0e6
3.5e6
3.0e6
2.5e6
2.0e6
1.5e6
1.0e6
5.0e5
0.0
160
180
200
220
240
260
280
300
320
258.0
286.0
330.0
188.8
152.8
173.8
193.8
201.8
222.0
237.8
246.0
270.6
284.4
162.0
181.8
194.0
202.0
210.0
222.0
226.0
236.0
246.0
260.0
286.0
330.0

Figure 1

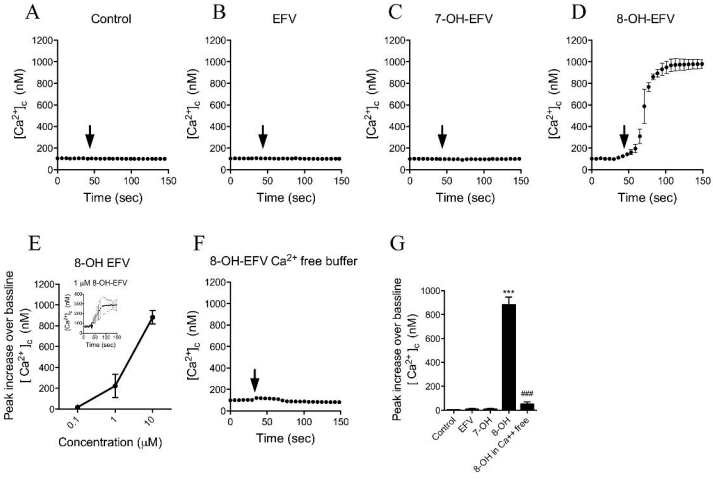
A
Control
B
EFV
C
7-OH-EFV
D
8-OH-EFV
[Ca2+]i (nM)
Time (sec)
E
8-OH EFV
Peak increase over bassline
[Ca2+]i (nM)
Concentration (μM)
1 μM 8-OH-EFV
F
8-OH-EFV Ca2+ free buffer
G
Peak increase over bassline
[Ca2+]i (nM)
***
####
Control
EFV
7-OH
8-OH
8-OH in Ca++ free

Figure 2

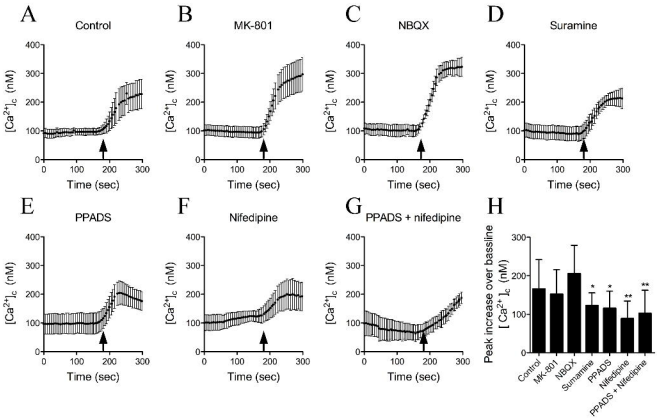
A
Control
B
MK-801
C
NBQX
D
Suramine
E
PPADS
F
Nifedipine
G
PPADS + nifedipine
H
[Ca2+]c (nM)
Time (sec)
Peak increase over bassline [Ca2+]c (nM)
Control
MK-801
NBQX
Suramine
PPADS
Nifedipine
PPADS + Nifedipine

Figure 3

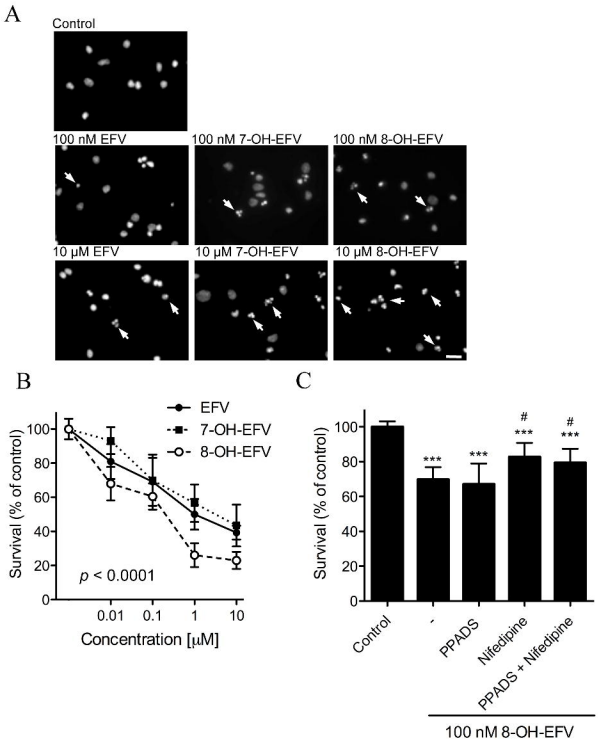
A
Control
100 nM EFV
100 nM 7-OH-EFV
100 nM 8-OH-EFV
10 µM EFV
10 µM 7-OH-EFV
10 µM 8-OH-EFV
B
EFV
7-OH-EFV
8-OH-EFV
Survival (% of control)
p < 0.0001
Concentration [µM]
C
Survival (% of control)
Control
PPADS
Nifedipine
PPADS + Nifedipine
100 nM 8-OH-EFV

Figure 4

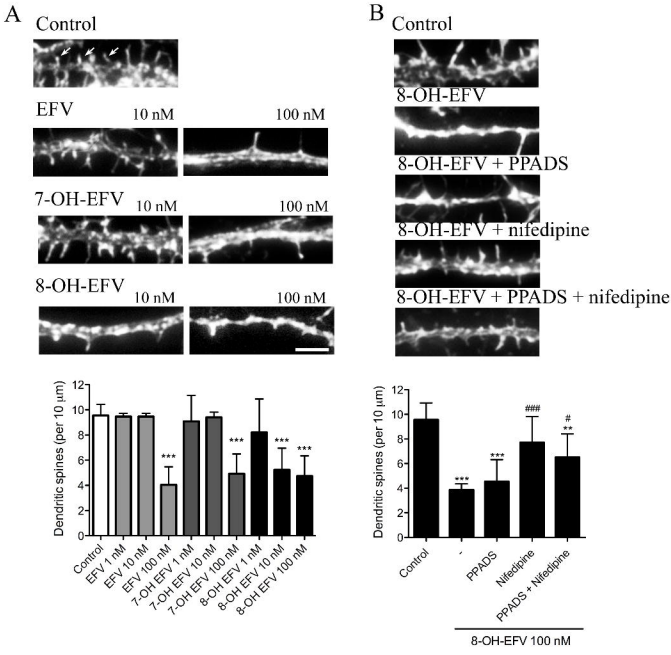
A
Control
EFV
10 nM
100 nM
7-OH-EFV
10 nM
100 nM
8-OH-EFV
10 nM
100 nM
Dendritic spines (per 10 µm)
Control
EFV 1 nM
EFV 10 nM
EFV 100 nM
7-OH EFV 1 nM
7-OH EFV 10 nM
7-OH EFV 100 nM
8-OH EFV 1 nM
8-OH EFV 10 nM
8-OH EFV 100 nM
B
Control
8-OH-EFV
8-OH-EFV + PPADS
8-OH-EFV + nifedipine
8-OH-EFV + PPADS + nifedipine
Dendritic spines (per 10 µm)
Control
PPADS
Nifedipine
PPADS + Nifedipine
8-OH-EFV 100 nM

Figure 5

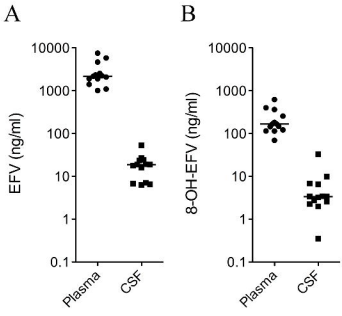

Figure 6